Journal of Applied Polymer Science

Montmorillonite Reinforced Type A Gelatin Nanocomposites

Silvia Panzavolta, Michela Gioffrè, Barbara Bracci, Katia Rubini, Adriana Bigi
Department of Chemistry "G. Ciamician," University of Bologna, via Selmi 2 40126 Bologna, Italy
Correspondence to: S. Panzavolta (E-mail: silvia.panzavolta@unibo.it)

ABSTRACT: This study investigates the structural, morphological, thermal, and mechanical properties of type A gelatin/montmorillonite (MMT) films as a function of MMT concentration. The variations of the X-ray diffraction pattern suggest that the structure of the nanocomposites turns from intercalated to exfoliated on increasing clay loading up to 20 wt %. Simultaneously, gelatin interaction with clay negative sheets during gelling provokes a reduction of the triple helix content of the composite films, in agreement with the reduction of the relative intensity of the 1.1 nm diffraction reflection of gelatin and of the values of denaturation enthalpy. On the other hand, the increase of the denaturation and decomposition temperatures, the significant rise of the Young's modulus, as well as the swelling decrease observed as clay content increases, demonstrate a relevant stabilizing effect of MMT on gelatin. The reinforcement action of MMT allows to utilize a relatively low concentration of the crosslinking agent genipin to further stabilize the films. The synergic action of clay and genipin prevents dissolution of the nanocomposites in aqueous solution and enhances their mechanical properties. © 2013 Wiley Periodicals, Inc. J. Appl. Polym. Sci. **2014**, *131*, 40301.

KEYWORDS: clay; biopolymers and renewable polymers; composites; films; mechanical properties

Received 12 June 2013; accepted 14 December 2013
DOI: 10.1002/app.40301

INTRODUCTION

Biohybrid nanostructured materials obtained by the assembly of polymers and inorganic solids are of remarkable interest due to the potential improvement of polymer properties—including enhanced mechanical strength, weight reduction, increased heat resistance, and improved barrier properties[1]—and the variety of possible applications, from regenerative medicine to advanced functional materials.[2] In particular, bionanocomposites, which are composed of biopolymers and inorganic solids characterized by at least one dimension at the nanometer range,[2] mimic the strategies utilized by Nature to synthesize high performance composite materials.[3,4] Among the inorganic solids, the expanding 2 : 1 type layer silicates received particular attention due to their low cost, ability to intercalate a huge number of compounds,[1,5,6] and to improve functional properties of biopolymers while preserving their biocompatibility,[2,7,8] as well as easiness of bionanocomposite preparation. Sodium montmorillonite (Na^+-MMT) is widely used as nanofiller because of its natural abundance and high aspect-ratio (about 1 nm thick by 100–1000 nm diameter sheet).[9] Furthermore, it is toxin-free and it displays widespread applications in medicine as well as in tissue engineering.[10,11]

Gelatin, which is obtained by chemical–thermal degradation of collagen is one of the most employed biopolymers. The numerous applications of gelatin range from packaging to health care, thanks to its biodegradability, excellent biocompatibility, plasticity, adhesiveness, abundance, and low cost. Furthermore, gelatin is non-immunogenic and non-carcinogenic, and it displays low antigenicity. In particular, gelatin-based films are thin, flexible, and transparent biodegradable materials, useful in engineering food, packaging, drug recover, and other applications.[12,13] The main drawback of gelatin as a material is its poor mechanical performance. Mechanical properties can be improved through crosslinking[14–18] or by combining the biopolymer with an inorganic filler. The surfaces of the clay sheets in MMT have an overall negative charge, which is balanced by the exchangeable Na^+ cations in the space between the sheets. Therefore, positively charged macromolecules can replace Na^+ ions and interact with the negative sheets via associative mechanism.[19,20] It follows that interaction with gelatin is promoted at pH values lower than the isoelectric point (pI) of the biopolymer.[21,22] Moreover, a highly charged MMT surface can polarize gelatin molecules and promote favorable associative interaction even when both have the same charge sign.[23]

Previous studies on gelatin–MMT bionanocomposites were mostly performed using type B bovine gelatin or fish gelatin.[1,20–27] In particular gelatin–MMT films were reported to show improved water resistance and water vapor permeability, as well as enhanced elastic modulus, with respect to pure gelatin films.[27,28] However, the high solubility of gelatin, which is its

main drawback, still limits the possible application of clay bionanocomposites.

With respect to type B gelatin, type A gelatin has a higher pI and its solutions have pH values below pI, which should promote interaction with clay sheets. Type A gelatin and MMT bionanocomposites have been investigated just at low relative gelatin content, namely 33% and 50%, (which gave intercalated and delaminated systems, respectively).[29] Herein, we report the results of a study carried out on nanocomposite films constituted of type A gelatin enriched with increased amounts of MMT, from 5% to 20%, with the aim to investigate the influence of clay on the structural and mechanical properties of gelatin and to explore the possibility to use MMT to stabilize the nanocomposites and reduce the concentration of crosslinking agent necessary to avoid dissolution in aqueous solution. The results show that a low concentration of a natural crosslinking agent, genipin, enhanced the beneficial effect of MMT on improving the mechanical properties and reducing the swelling of the films.

MATERIALS AND METHODS

Type A gelatin (280 Bloom, Italgelatine S.p.A.) from pig skin and clay MMT Nanofil 116 (Southern Clay Products) were used.

Gelatin films (GEL) were prepared from 5% (w/v) aqueous gelatin solutions. About 10 mg of sodium azide was added to prevent bacteriological degradation. The films were obtained by pouring 10 mL of gelatin solution on the bottom of Petri dishes (diameter of 6 cm) and air-drying at room temperature. The same procedure was utilized for the preparation of the nanocomposite films, which were obtained by mixing 20 mL of aqueous gelatin solution, containing 2 g of gelatin, with 20 mL of aqueous suspensions at different MMT content under stirring. Clay content was varied in order to obtain suspensions containing 5%, 15%, or 20% w/w of MMT with respect to gelatin. Before mixing, clay suspensions were submitted to ultrasonication for 20 min. Now onward, the composite films will be labeled MMTX, where X indicates MMT percentage in the sample. The pH values of the GEL/MMT suspensions were around 7.

Some samples were crosslinked with genipin (Wako, Japan). A volume of 10 mL of 0.15% genipin in 0.1*M* phosphate buffered saline solution (PBS) at pH 7.4, was poured onto the dried films in the Petri dishes.[18] After 24 hr at 25°C, the genipin solution was removed and substituted with an equal volume of 0.1*M* glycine for an hour, to remove the excess of genipin. Finally, the films were repeatedly washed with double distilled water and air-dried at room temperature. Crosslinked samples were labeled C-MMTX.

Characterization

X-ray diffraction (XRD) analysis was carried out by means of a Panalytical XCelerator powder diffractometer. Cu$K\alpha$ radiation was used (40 mA, 40 kV). The 2θ range was from 3° to 50° with a step size of 0.033° and time/step of 20 s.

Stress–strain curves were recorded using an INSTRON Testing Machine 4465 and the Series IX software package. Strip-shaped samples (3 × 30 mm) of air-dried films were stretched using a crosshead speed of 5 mm/min. The thickness of the samples was determined using a micrometer. Crosslinked samples were tested in rehydrated conditions: strip-shaped films were immersed in a solution of water and ethanol in a 2 : 3 ratio (constant relative humidity of 75%) for 72 hr and stretched in a mixture of the same composition with the same crosshead speed. The thickness of the samples was determined using a Leitz SM-LUX-POL microscope. The stress–strain curves were used to measure the Young's modulus, E, the stress at break, σb, and the strain at break, εb. Duncan's Multiple Range Test was used to detect differences among film property mean values.

Data are reported as mean ± standard deviations (SD) at a significance level of $P < 0.05$.

Fourier transform infrared (FT-IR) spectra were collected with a Thermo Nicolet 380 spectrometer equipped with ATR accessory and the spectra resolution was 4 cm^{-1}. The spectrum of the sample was obtained by placing a film onto germanium crystal without any additional sample preparation. The spectra were the result of 196 scans.

Calorimetric measurements were performed using a Perkin Elmer Pyris Diamond differential scanning calorimetry (DSC) equipped with a model ULSP intracooler. Temperature and enthalpy calibration were performed using high-purity standards (*n*-decane and indium). Samples were examined in air-dried conditions. Heating was carried out at 5°C/min from 40°C to 130°C. Denaturation temperature (T_D) was determined as the peak value of the corresponding endothermic event. The value of denaturation enthalpy was calculated with respect to the weight of air-dried gelatin.

Thermogravimetric analysis (TGA) was carried out using a Perkin Elmer TGA-7. Heating was performed in a platinum crucible in air flow (20 mL/min) at a rate of 10°C/min up to 800°C. The samples weights were in the range 5–10 mg.

For swelling measurements, gelatin and gelatin–MMT films were weighted in air-dried conditions and immersed in 0.1*M* PBS solution at pH 7.4. At selected times, ranging from 1 to 1400 min, wet samples were removed from PBS solution, wiped with filter paper to eliminate excess liquid and weighed. The amount of adsorbed water was calculated as:

$$W\% = \frac{(W_w - W_d) \times 100}{W_d}$$

where W_w and W_d are, respectively, the weights of the wet and the air-dried samples.

Morphological investigation of fracture surfaces of the dried gelatin–MMT composite films was performed using a Philips XL-20 scanning electron microscope (SEM) operating at 15 kV. The samples were sputter-coated with gold prior to examination.

RESULTS AND DISCUSSION

The presence of clay in the nanocomposites influences the microstructure of the films, as it results from SEM investigation carried out on samples fractured in the direction orthogonal to the surface. The images of the fractured surface show that the

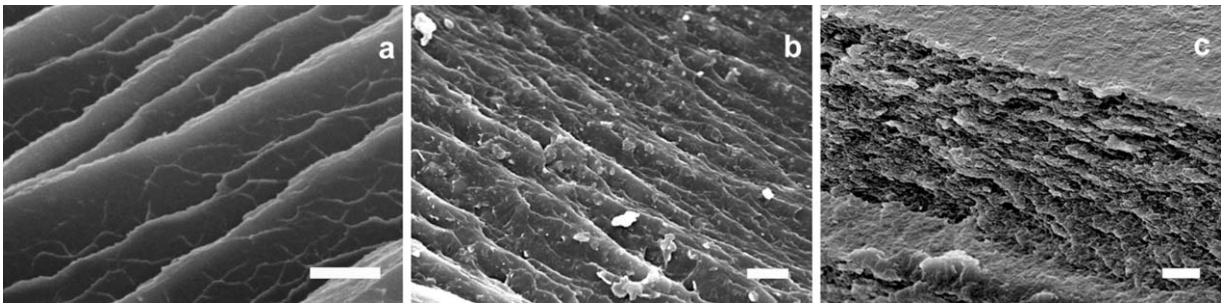

Figure 1. SEM images of the fractured surfaces of nanocomposites: (**a**) GEL, (**b**) MMT5, and (**c**) MMT15. Bars = 5 μm.

inner region of pure gelatin films is organized in regular layers parallel to the film surface [Figure 1(a)]. The composites still display a layered organization, although less regular than that of pure gelatin. The effect of clay on film morphology is evident already at low concentration [Figure 1(b)], and it increases at high MMT content [Figure 1(c)]. Film thickness increases with increasing MMT content, from a mean value of about 100 μm measured for GEL samples up to about 160 μm for MMT20.

The XRD patterns of pristine MMT and type A gelatin film are reported in Figure 2. The XRD pattern of gelatin shows a reflection at about 8° of 2θ, corresponding to a periodicity of about 1.1 nm, which is associated to the diameter of the collagen triple helix, and a broad peak in the range 12°–30° of 2θ, which is related to peptide bonds. It was previously shown that the integrated intensity of the 1.1 nm reflection can be used as a measure of the triple-helix content of gelatin films.[16,30] The main feature of the XRD pattern of MMT (Figure 2) is the presence of the (001) reflection at about 7.05° of 2θ, corresponding to the characteristic silicate interlayer spacing of 1.25 nm.[24] The shift of the (001) reflection at smaller angles in the nanocomposites (Figure 3) indicates an enlargement of the basal spacing of MMT, possibly due to the insertion of gelatin molecules between MMT layers.[31] Moreover, the relative intensity of the MMT (001) reflection decreases significantly on increasing clay content of the composites, and it is no longer appreciable in the pattern of MMT20. It can be suggested that the lack of the (001) reflection in the pattern of the samples at relatively high MMT content is indicative of the transition from an intercalated to an exfoliated structure.[21,28] Simultaneously, the addition of clay into the nanocomposites provokes a reduction of the relative intensity of the 1.1 nm reflection of gelatin, which cannot be justified by the relatively small reduction of gelatin relative

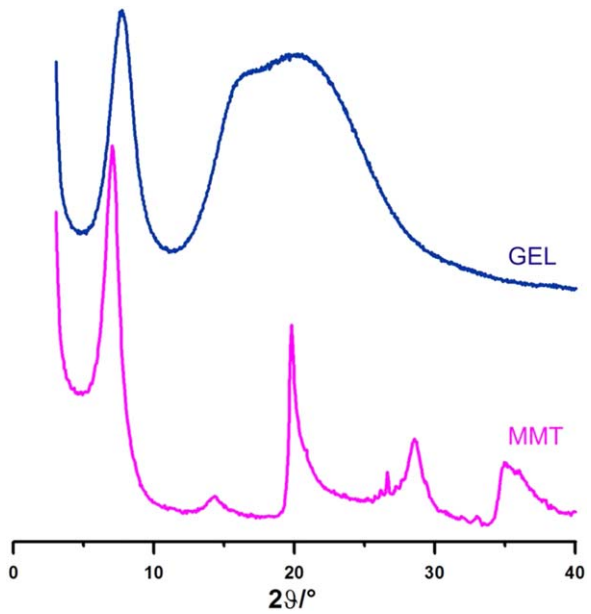

Figure 2. XRD pattern of gelatin film and MMT powder. [Color figure can be viewed in the online issue, which is available at wileyonlinelibrary.com.]

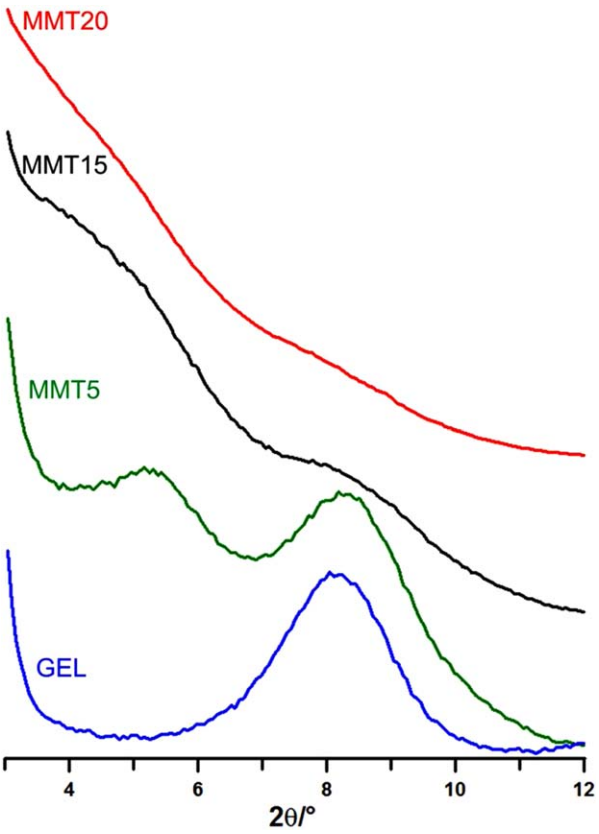

Figure 3. XRD patterns of GEL/MMT nanocomposites at different MMT content. [Color figure can be viewed in the online issue, which is available at wileyonlinelibrary.com.]

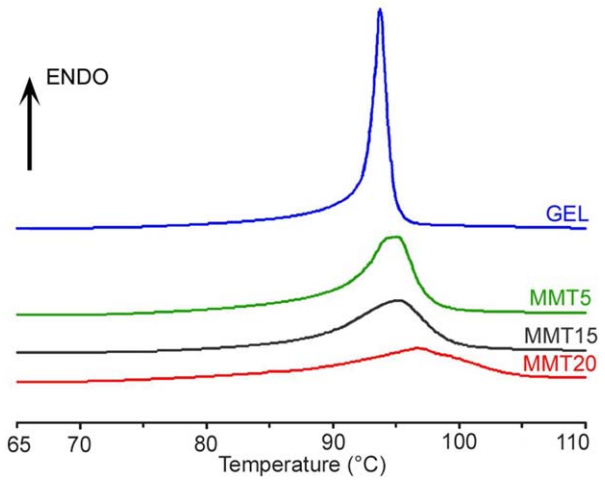

Figure 4. Typical DSC curves of the nanocomposite films at different MMT content. [Color figure can be viewed in the online issue, which is available at wileyonlinelibrary.com.]

amount in the composites. Renaturation of gelatin occurs during gelling: interaction with clay during this process would hinder gelatin recoil into the triple-helix structure, facilitating the penetration of the biopolymer into MMT interlayer space.[31] As a consequence, the renaturation level of gelatin decreases as MMT content increases. This hypothesis is supported by the results of DSC investigation. The DSC plot of collagenous materials exhibits an endothermic peak due to the helix–coil transition of collagen. The value of the denaturation enthalpy associated to this peak is related to the relative amount of triple-helical structure in the samples, and it is significantly lower for gelatin with respect to collagen.[30] Figure 4 reports the DSC plots of dry nanocomposites at different MMT content. It is evident that the denaturation peak shifts to higher temperature on increasing MMT content, as shown by the values of denaturation temperature, T_D (Table I). The variation of thermal stability of gelatin films as a function of composition is confirmed by the results of TGA. The thermogravimetric plot of gelatin displays three thermal processes: the first one occurs between 25°C and about 250°C, and it is due to loss of water; the second one between 250°C and 450°C involves gelatin decomposition, and the third one between 450°C and 700°C corresponds to the combustion of the residual organic component.[32] The experimental TG curves reported in Figure 5 shows that the presence of clay provokes a delay in the second weight loss corresponding to decomposition of the protein, in agreement with increase of the initial temperature of mass loss (T_0)

Table I. Denaturation Temperature, T_D, and Denaturation Enthalpy, ΔH_D, of Nanocomposite Films at Different MMT Content

Sample	T_D (°C)	ΔH_D (J/g)
GEL	94 ± 1	32 ± 1
MMT5	95 ± 1	28 ± 1
MMT15	96 ± 1	18 ± 1
MMT20	97 ± 1	17 ± 1

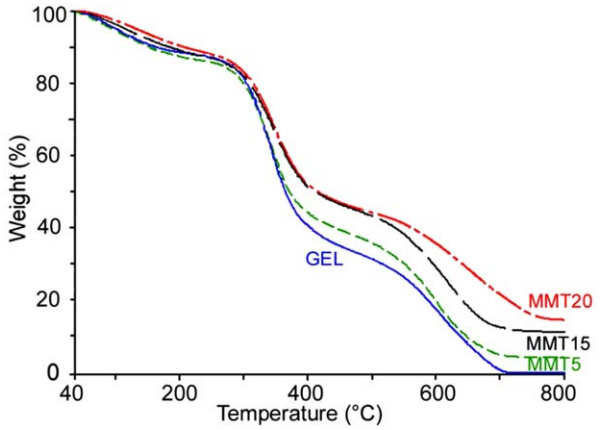

Figure 5. TG curves of the nanocomposite films at different MMT content. [Color figure can be viewed in the online issue, which is available at wileyonlinelibrary.com.]

and the temperature of maximum rate of mass loss (T_{max}) reported in Table II. The final residue at 800°C is in good agreement with MMT original content. At variance with T_D, the values of denaturation enthalpy, ΔH_D, decrease as clay content increases (Table I). The values obtained for the samples MMT20 are <60% of those of pure gelatin, confirming a drastic decrease of the renaturation level of the protein in the nanocomposites.

Figure 6 reports a comparison between the FT-IR spectrum of pure gelatin film and those of MMT5 and MMT20 in the 1800–1000 cm^{-1} amide region. The amide I band occurs in the 1660–1620 cm^{-1} region and it is associated with the carbonyl C═O double stretching mode. The amide II band, in the 1550–1520 cm^{-1} region, has been ascribed to the deformation of N—H bonds and C—H stretching, whereas amide III corresponds to vibration in the plane of C—N and N—H groups of bound amide or vibration of CH_2.[33] The spectra reported in Figure 6 display a reduction of the relative intensity of the amide absorption bands on increasing clay content of the samples, which is a further indication of the decrease of triple-helix content of gelatin.[34] Moreover, the FT-IR amide bands in the spectrum of MMT20 show some splitting, which was previously ascribed to H bond interaction between hydrogen atoms of gelatin peptide bonds and oxygen atoms from free OH and Si—O—Si groups in MMT.[27]

Table II. Temperature Corresponding to Initial of Mass Loss (T_0) and Temperature of Maximum Rate of Mass Loss (T_{max}) of the Second Weight Loss Present in the TG Curves of the Different Samples, Together with the Final Residue at 800°C (Wt %)

	Second stage		
Sample	T_0 (°C)	T_{max} (°C)	Residue at 800°C (wt %)
GEL	223	343	0
MMT5	234	344	4
MMT15	238	350	14
MMT20	241	349	18

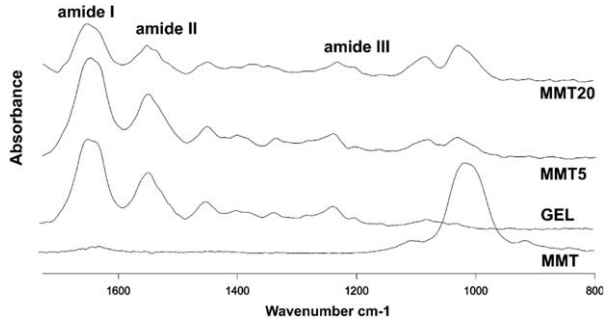

Figure 6. FT-IR spectra of MMT, pure gelatin film, MMT5, and MMT20 nanocomposites.

The reduction of the triple-helix content should provoke a worsening of the mechanical properties of the nanocomposites.[30] On the contrary, the mechanical properties of the films improve on increasing clay content, indicating that MMT acts as reinforcement for gelatin. Stress–strain curves recorded from air dried samples were used to evaluate the Young's modulus, E, the stress at break, σ_b, and the deformation at break, ε_b, of the films. The results reported in Table III show that variation in composition does not significantly affect the stress at break, σ_b, whereas it provokes a modest but significant decrease of the deformation at break, ε_b, in the samples at relatively high MMT content. Moreover, the Young's modulus, E, undergoes a remarkable improvement on increasing clay content, beyond MMT5. In fact, MMT20 exhibits a 215% increase with respect to pure gelatin. The observed increase of the Young's modulus is similar to that observed from Fernandes et al.[29] for type A gelatin nanocomposites at 50% clay loading and significantly higher than that previously reported for type B bovine gelatin/clay nanocomposites.[21] These results are in agreement with the stronger interactions between type A gelatin chains and MMT sheets as expected on the basis of the higher pI of type A gelatin with respect to type B gelatin. At variance with type B gelatin, type A gelatin solutions display pH values below pI, therefore the biopolymer is positively charged, which enhances interaction with the negatively charged clay sheets.

The presence of MMT reduces the degree of swelling of the nanocomposites, as it can be observed from the comparison between pure gelatin and MMT20 reported in Figure 7. Swelling of pure gelatin is quite fast: it reaches values >1000% in a few hours and it exceeds 1600% in 15 hr. On the contrary, the degree of swelling of MMT20 after 15 hr in PBS solution is just a bit above 1000%.

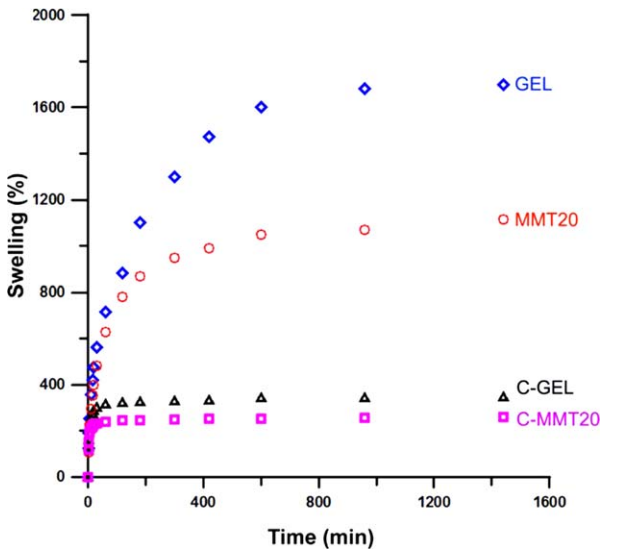

Figure 7. Swelling curves of the nanocomposite films at different MMT content. [Color figure can be viewed in the online issue, which is available at wileyonlinelibrary.com.]

The reduction of swelling due to the presence of clay, although significant, is not sufficient to prevent gelatin dissolution. Both gelatin and the nanocomposites dissolve completely after a few days in PBS solution. In fact, gelatin is highly soluble in aqueous solution, and gelatin materials for long-term applications must be submitted to crosslinking, which improves both the thermal and the mechanical stability of the material.[18] Herein we used a naturally occurring crosslinking agent, genipin, which can be obtained from an iridoid glucoside, geniposide, abundantly present in gardenia fruits.[35] In view of the reinforcement action of MMT, which contributes to swelling reduction, a low concentration of genipin, namely 0.15 wt % was chosen to crosslink the nanocomposites. The results indicate that crosslinking remarkably reduces the degree of swelling of both pure gelatin and nanocomposite films, even at this low genipin concentration. Figure 7 reports the swelling curves of crosslinked gelatin and MMT20, intermediate curves were observed for the nanocomposites at lower clay content. The degree of swelling reached at 15 hr is below 400% for all the sample, and it is lower for the nanocomposites than for gelatin. Swelling

Table III. Strain at Break, ε_b, Stress at Break, σ_b, and Young's Modulus, E, of Gelatin and MMT–Gelatin Composite Films Tested in Dry Conditions

Sample	σ_b (MPa)	E (GPa)	ε_b (%)
GEL	79 ± 9	2.1 ± 0.3	14 ± 4
MMT5	85 ± 5	1.8 ± 0.5	18 ± 4
MMT15	86 ± 9	3.7 ± 0.5[c]	11 ± 2[b]
MMT20	82 ± 8	4.5 ± 0.5[a,c]	8 ± 2[a,c]

ε_b: [a] MMT20 vs. GEL $P < 0.05$; [b] MMT15 vs. MMT5 $P < 0.01$; [c] MMT20 vs. MMT5 $P < 0.001$.
E: [c] MMT20, MMT15 vs. GEL, MMT5 $P < 0.001$; [a] MMT20 vs. MMT15 $P < 0.05$.

Table IV. Strain at Break, ε_b, Stress at Break, σ_b, and Young's Modulus, E, of Crosslinked Gelatin and Composite Films, Examined at RH = 75%

Sample	σ_b (MPa)	E (MPa)	ε_b (%)
C-GEL	0.80 ± 0.31	1.51 ± 0.10	39 ± 8
C-MMT5	1.30 ± 0.46	2.59 ± 0.37	42 ± 10
C-MMT15	1.12 ± 0.34	3.75 ± 0.38[c]	29 ± 8
C-MMT20	1.11 ± 0.31	4.47 ± 0.29[b,c]	36 ± 10

E: [c] MMT20, MMT15 vs. GEL $P < 0.001$; [c] MMT20, MMT15 vs. MMT5 $P < 0.001$; [b] MMT20 vs. MMT15 $P < 0.01$.

reduction due to genipin crosslinking allowed to record the stress–strain curves of the films in rehydrated conditions. The Young's modulus, E, the stress at break, σ_b, and the deformation at break, ε_b, of crosslinked samples are reported in Table IV. The values of the mechanical parameters obtained for pure gelatin are in agreement with previous data obtained on gelatin films crosslinked in the same conditions.[18] Moreover, the data reported in Table IV put into evidence the synergic effect of clay reinforcement on the improvement of the mechanical properties of the crosslinked nanocomposites. As a matter of fact, the values of Young's modulus, E, increase on increasing MMT content up to 4.47 ± 0.29 MPa for MMT20, that is about 300% of the value of crosslinked gelatin.

CONCLUSIONS

Type A gelatin/MMT nanocomposites display enhanced thermal stability and mechanical properties, as well as reduced swelling with respect to gelatin films, indicating a stabilizing role of MMT on gelatin. The interaction of gelatin molecules with clay sheets during gelling interferes with the renaturation process of gelatin, provoking a reduction of the triple-helix content of the nanocomposites as a function of clay relative amount. Nonetheless, the reinforcement action of MMT accounts for the increased values of the denaturation and decomposition temperatures, as well as of the Young's modulus, while it decreases swelling. Moreover, its presence allows to utilize a reduced concentration of crosslinking agent to stabilize the nanocomposites.

ACKNOWLEDGMENTS

This research was carried out with the financial support of the University of Bologna.

REFERENCES

1. Ray, S. S.; Okamoto, M. *Prog. Polym. Sci.* **2003**, *28*, 1539.
2. Ruiz-Hitzky, E.; Aranda, P.; Darder, M.; Ogawa, M. *Chem. Soc. Rev.* **2011**, *40*, 801.
3. Pinnavaia, T. J.; Beall, G. Polymer–Clay Nanocomposites; John Wiley & Sons: New York, **2000**.
4. Ruiz-Hitzky, E.; Darder, M.; Aranda, P. In Bio-inorganic Hybrid Nanomaterials: Strategies Syntheses Characterization and Applications; Ruiz-Hitzky, E.; Ariga, K.; Lvov, J. M., Eds.; Wiley-VCH: Weinheim, **2007**.
5. Ruiz-Hitzky, E.; Darder, M.; Aranda, P. *J. Mater. Chem.* **2005**, *15*, 3650.
6. Giannelis, E. P. *Adv. Mater.* **1996**, *8*, 29.
7. Ruiz-Hitzky, E.; Aranda, P.; Darder, M.; Rytwo, G. *J. Mater. Chem.* **2010**, *20*, 9306.
8. Darder, M.; Aranda, P.; Ruiz, A. I.; Fernandes, F. M.; Ruiz-Hitzky, E. *Mater. Sci. Technol.* **2008**, *24*, 1100.
9. Podsiadlo, P.; Kaushik, A. K.; Arruda, E. M.; Waas, A. M.; Shim, B. S.; Xu, J.; Nandivada, H.; Pumplin, B. G.; Lahann, J.; Ramamoorthy, A.; Kotov, N. A. *Science* **2007**, *318*, 80.
10. Baker, S. E.; Sawvel, A. M.; Zheng, N.; Stucky, G. D. *Chem. Mater.* **2007**, *19*, 4390.
11. Vaiana, C. A.; Leonard, M. K.; Drummy, L. F.; Singh, K. M.; Bubulya, A.; Vaia, R. A.; Naik, R. R.; Kadakia, M. P. *Biomacromolecules* **2011**, *12*, 3139.
12. Bergo, P.; Sobral, P. J. A. *Food Hydrocolloids* **2007**, *21*, 1285.
13. Boanini, E.; Bigi, A. *J. Colloid. Interf. Sci.* **2011**, *362*, 594.
14. Bigi, A.; Bracci, B.; Cojazzi, G.; Panzavolta, S.; Roveri, N. *Biomaterials* **1998**, *19*, 2335.
15. Bae, H. J.; Darby, D. O.; Kimmel, R. M.; Park, H. J.; Whiteside, W. S. *Food Chem.* **2009**, *114*, 180.
16. Boanini, E.; Rubini, K.; Panzavolta, S.; Bigi, A. *Acta Biomater.* **2010**, *6*, 383.
17. Fakirov, S.; Sarac, Z.; Anbar, T.; Boz, B.; Bahar, I.; Evstatiev, M.; Apostolov, A. A.; Mark, J. E.; Kloczkowski, A. *Colloid. Polym. Sci.* **1997**, *275*, 307.
18. Bigi, A.; Cojazzi, G.; Panzavolta, S.; Roveri, N.; Rubini, K. *Biomaterials* **2002**, *23*, 4827.
19. Lin, J. J.; Chu, C. C.; Chiang, M. L.; Tsai, W. C. *J. Phys. Chem. B* **2006**, *110*, 18115.
20. Taheri, Q. N.; Bolisetty, S.; Adamcik, J.; Mezzenga, R. *Biomacromolecules* **2012**, *31*, 2136.
21. Zheng, J. P.; Li, P.; Ma, Y. L.; De Yao, K. *J. Appl. Polym. Sci.* **2002**, *86*, 1189.
22. Bae, H. J.; Hyun, J.; Park, H. J.; Hong, S. I.; Byun, Y. J.; Darby, D. O.; Kimmel, R. M.; Whiteside, W. S. *Food Sci. Technol.* **2009**, *42*, 1179.
23. Dobrynin, A. V.; Rubinstein, M.; Joanny, J. F. *Macromolecules* **1997**, *30*, 4332.
24. Zheng, J. P.; Wang, C. Z.; Wang, X. X.; Wang, H. Y.; Zhuang, H.; De Yao, K. *React. Funct. Polym.* **2007**, *67*, 780.
25. Zhuang, H.; Zheng, J.; Gao, H.; De Yao, K. *J. Mater. Sci. Mater. Med.* **2007**, *18*, 951.
26. Jang, S. A.; Lim, G. O.; Song, K. B. *Int. J. Food Sci. Technol.* **2010**, *45*, 1883.
27. Martucci, J. F.; Ruseckaite, R. A. *Polym. Plast. Technol. Eng.* **2010**, *49*, 581.
28. Rao, Y. Q. *Polymer* **2007**, *48*, 5369.
29. Fernandes, F. M.; Ruiz, A. I.; Darder, M.; Aranda, P.; Ruiz-Hitzky, E. *J. Nanosci. Nanotechnol.* **2009**, *9*, 221.
30. Bigi, A.; Panzavolta, S.; Rubini, K. *Biomaterials* **2004**, *25*, 5675.
31. Talibudeen, O. *Faraday Soc.* **1955**, *51*, 582.
32. Bigi, A.; Panzavolta, S.; Rubini, K. *Chem. Mater.* **2004**, *16*, 3740.
33. Hashim, D. M.; Che Man, Y. B.; Norakasha, R.; Shuhaimi, M.; Salmah, Y.; Syahariza, Z. A. *Food Chem.* **2010**, *118*, 856.
34. Muyonga, J. H.; Cole, C. G. B.; Duodu, K. G. *Food Hydrocolloids* **2004**, *18*, 581.
35. Sung, H. W.; Liang, I. L.; Chen, C. N.; Huang, R. N.; Liang, H. F. *J. Biomed. Mater. Res.* **2001**, *55*, 538.